

Fig. 3 Compressibility corrections to incompressible C_p distribution.

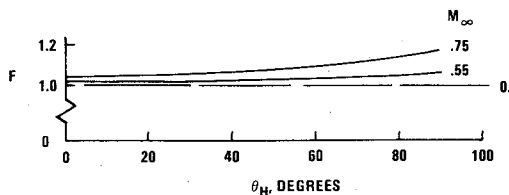


Fig. 4 Compressibility correction factor F .

theoretical stagnation point values from Eq. (1). The agreement between the latter and the coefficient A is quite good and substantiates both the data and the curve fit, Eq. (2). Figure 3 and Eq. (2) provide then the basis for the compressibility correlation described below.

The location of any point on the hemispherical portion of the turret can be defined by a single coordinate θ_T representing the included angle between the radius passing through the point and one passing through the point P (Fig. 1). Because of the asymmetry of the turret, C_p may not be identical for a given θ_T , (see rays A and E in Fig. 2) although the differences are small. We assume, however, that the angle θ_T has a single corresponding location θ_H on Hsieh's axisymmetric model. This implies that although C_p varies slightly for a given θ_T , the compressibility correction is the same and is defined by its value at θ_H . We define a correction factor F as

$$F_H(\theta_H, M_\infty) = \left(\frac{P/P_\infty(\theta_H, M_\infty)_c}{P/P_\infty(\theta_H)_i} \right)_{\text{Hsieh}} \quad (3)$$

where subscripts c and i denote the compressible and incompressible conditions, respectively. From the potential flow solution to the turret flowfield we find C_{p_i} and evaluate $P/P_\infty(\theta_T)_i$ from Eq. (1). Since we assume that $F_H(\theta_H, M_\infty) = F_T(\theta_T, M_\infty)$, the compressibility corrected pressure ratio is given then by

$$P/P_\infty(\theta_T, M_\infty)_c = F_H(\theta_H, M_\infty) P/P_\infty(\theta_T)_i \quad (4)$$

and finally, $C_{p_c}(\theta_T, M_\infty)$ is found from Eq. (1). The factor F has been plotted vs θ_T in Fig. 4 which shows that, for the indicated Mach number range, the effect of compressibility on P is small. The compressibility corrected C_p distribution is plotted in Fig. 2 where it is shown to have the proper trend and magnitude and to provide excellent agreement with the data.

Summary

It has been shown that a reasonable estimate of the turret C_p distribution in the region of attached flow is provided using an incompressible, inviscid code, which was successful in rationalizing the results of wind tunnel test measurements and which accounts for the effects of the turret configuration. In particular, for the M_∞ range considered here, compressibility effects were found to be small. However, an improved agreement between data and analysis is obtained using the code together with a compressibility correction proposed in this report.

Acknowledgment

This work supported by the USAF Weapons Laboratory, Kirtland AFB, under Contract F2960-79-C-0010.

References

- ¹ Proceedings of the Aero-Optics Symposium on Electromagnetic Wave Propagation from Aircraft, NASA Conference Publication 2121, April 1980.
- ² Steenken, W.G., "Wind Tunnel Investigation of 0.3-Scale APT Closed-Port Turret and Fairing Model," Convair Aerospace Division of General Dynamics, Report FZA-458-2, Jan. 1973.
- ³ Laderman, A.J., "Surface Pressure Distribution Over an Airborne HEL Turret," Ford Aerospace and Communications, Newport Beach, Calif., FACC Report U-6680, March 1981.
- ⁴ Hess, J.L. and Smith, A.M.O., "Calculation of Non-Lifting Body Potential Flow About Arbitrary Three Dimensional Bodies," McDonnell Douglas Report E.S. 40622, March 1962.
- ⁵ Hsieh, T., "Hemisphere-Cylinder in Transonic Flow, $M_\infty = 0.7 \sim 1.0$," *AIAA Journal*, Vol. 13, Oct. 1975, pp. 1411-1413.
- ⁶ Grabow, R.M., Ford Aerospace, private communication, 1981.

AIAA 82-4006

ADEN Plume Flow Properties for Infrared Analysis

Chong-Wei Chu* and Joe Der Jr.†
Northrop Corporation, Hawthorne, Calif.

IN Ref. 1 a simple modeling technique was presented to predict two-dimensional-nozzle plume properties for IR signature analysis. Models were developed and validated through comparisons with test data for two-dimensional converging-diverging (CD) and two-dimensional plug nozzles exhausting into quiescent air. The modeling technique was subsequently extended to an augmented deflecting exhaust nozzle (ADEN) with bypass ratios up to unity and with the engine swirl effectively accounted for in the model.² This Note presents the predicted plume properties for an ADEN [with a bypass ratio (BPR) of 0.25] with and without consideration of the engine swirl, and shows the striking effect of a 10-deg engine swirl[‡] on the plume total temperature distributions. Such effects were first recognized in Ref. 3.

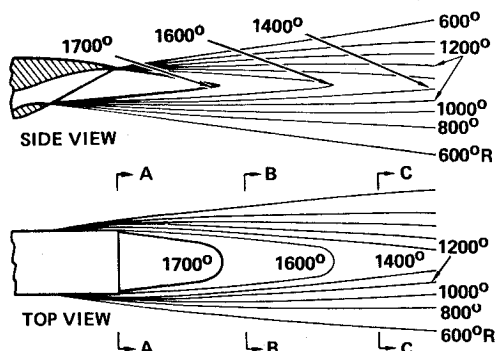
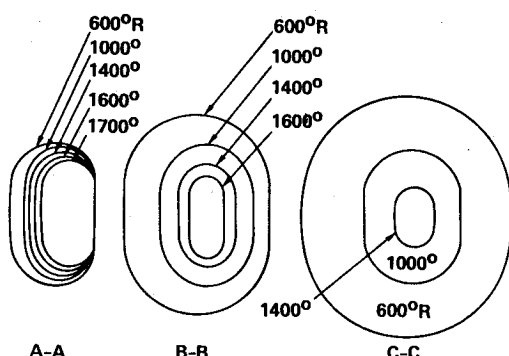
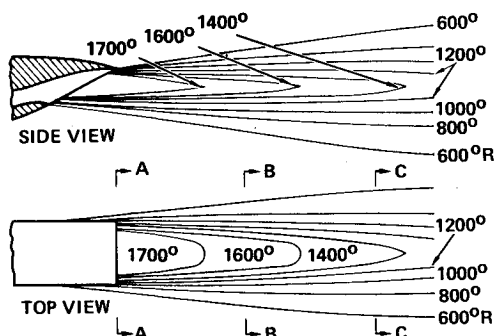
Figure 1 shows the predicted total temperature contours in the plume of an ADEN with a nozzle pressure ratio (NPR) of 2.76 and a zero bypass ratio and maximum exit total tem-

Received June 23, 1981. Copyright © American Institute of Aeronautics and Astronautics, Inc., 1981. All rights reserved.

*Senior Scientist, Department of Propulsion Research, Aircraft Division. Member AIAA.

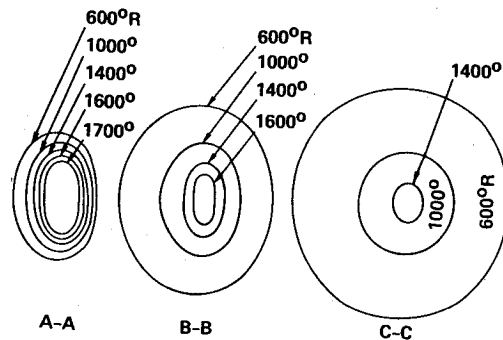
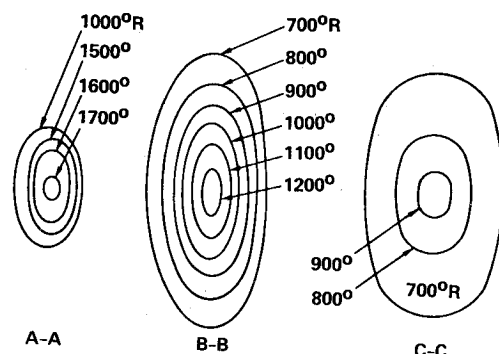
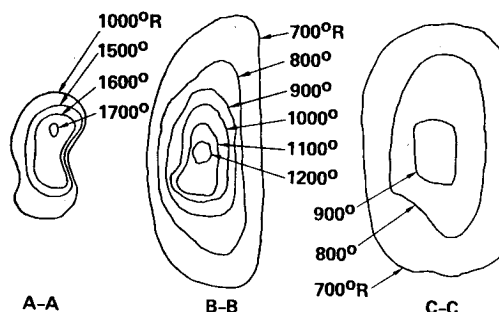
†Senior Technical Specialist, Department of Propulsion Research, Aircraft Division. Associate Fellow AIAA.

‡The swirl angle is defined as the arc tangent of the ratio between the swirl and axial velocities.

Fig. 1 Total temperature contours for ADEN; $NPR = 2.76$, $BPR = 0$.Fig. 2 Cross-sectional total temperature contours for ADEN; $NPR = 2.76$, $BPR = 0$.Fig. 3 Total temperature contours for ADEN; $NPR = 2.76$, $BPR = 0.25$.

perature of $1700^\circ R$, using the method of Ref. 2. Since the ADEN can be viewed as a two-dimensional nozzle with a slant exit, the plume of the ADEN resembles that of a two-dimensional CD nozzle, with the exception that at a given station the lower mixing layer is thicker than the upper mixing layer because of the difference in the distances available for external mixing. In the cross-sectional contour plots at three specified stations, A-A, B-B, and C-C, the differences of the mixing layer thickness are more easily visible (Fig. 2). When 25% of bypass air was added to the turbine exhaust while maintaining the same nozzle pressure ratio, some reduction of total temperature in the plume became evident, as shown by the predicted total temperature contours in Fig. 3 and the corresponding cross-sectional plots in Fig. 4. These figures show that a moderate amount of IR signature reduction can be expected from a low bypass ratio of 0.25.

However, when the engine swirl of $10 \text{ deg} \pm$ was accounted for in the model,² a dramatic reduction in total temperature was accomplished at stations B-B and C-C, where the maximum total temperature dropped 400 and $500^\circ F$,

Fig. 4 Cross-sectional total temperature contours for ADEN; $NPR = 2.76$, $BPR = 0.25$.Fig. 5 Predicted total temperature contours for ADEN ($NPR = 2.76$, $BPR = 0.25$) under the influence of engine swirl.Fig. 6 Measured total temperature contours for ADEN ($NPR = 2.76$, $BPR = 0.25$) in the presence of engine swirl.

respectively, as shown in Fig. 5. Physically, the reduction is due to a vigorous interchange of large volumes of hot and cold gases which is generated by a pair of corotating vortices. These two vortices are created when the swirl from the engine splits up as it passes through the rectangular throat and emerges from the lower edge of the exit.³ The result is that substantial mixing occurs within a short distance from the nozzle exit. (Note that the effect of engine swirl in an axisymmetric plume will be very much smaller: There is no reason for the swirl to break up into two, and a single swirling motion in an axisymmetric plume will not promote a large-scale interchange of fluid, although it will somewhat increase mixing due to shear.) To verify the prediction, General Electric's test data⁴ are presented in Fig. 6 for comparison. For contour plots, which can be sensitive to slight data discrepancies, the agreement is very good. Since the IR signature is a function of the fourth power of temperature, the effect of engine swirl on IR signature reduction is seen to be highly significant. Similar reductions are expected for other two-dimensional nozzles. Indeed, the concept of using the two-dimensional nozzle for IR signature reduction may depend on the effect of engine swirl. Recently, in the absence of engine swirl, a series of static tests on subscaled models,⁵

[§]This information was obtained from the Engine Cycle Deck for the GE YJ101.

using a heater-burner to simulate the engine exhaust, seemed to indicate that the two-dimensional CD nozzle with exit aspect ratios less than 10 would not produce less IR signature than the equivalent axisymmetric nozzle (see Fig. 67 of Ref. 5). The effect of the engine swirl is expected to be more important when external streams are present, since in such cases external mixing due to shear is otherwise reduced because of the lowered velocity differences between the plume and external stream.

In conclusion, a simple modeling technique has been developed^{1,2} to provide economical yet adequate prediction of two-dimensional-nozzle plume properties for IR signature analysis. Successful models were developed for ADEN, two-dimensional CD, and two-dimensional plug nozzles with and without bypass flow and/or engine swirl. A 10-deg engine swirl was found to reduce the predicted plume temperature dramatically. Therefore the inherent engine swirl, though undesirable from the performance point of view, appears to be highly effective in reducing the IR signature of a two-dimensional-nozzle plume.

Acknowledgments

This work was performed under Northrop IR&D program. The authors wish to thank Dr. Brian L. Hunt for his encouragement, discussion, and valuable suggestions.

References

- ¹ Chu, C.W., Der, J. Jr., and Wun, W., "A Simple 2D-Nozzle Plume Model for IR Analysis," AIAA Paper 80-1808, Aug. 1980.
- ² Chu, C.W. and Der, J. Jr., "Modeling of 2D-Nozzle Plume for IR Signature Prediction under Static Conditions," AIAA Paper 81-1108, June 1981.
- ³ Der, J. Jr., Chu, C.W., Hunt, B.L. and Lorincz, D.J., "Water-Tunnel Studies of Evolution of Engine Swirl in a 2D-Nozzle Plume," submitted to *Journal of Aircraft*.
- ⁴ "Advanced V/STOL Propulsion-Component Development," Nozzle Deflector Final Report, Vol. II, GE Rept. R77AEG441, General Electric Co., Aircraft Engine Group, Cincinnati, Ohio, Aug. 1977, Figs. 43-45.
- ⁵ Steven, H.L. and Herrick, P.W., "Installed Turbine Engine Survivability Criteria (ITESC) Program-Semiannual Interim Technical Report No. 5," United Technologies Corp., Pratt & Whitney Aircraft Group, West Palm Beach, Florida, FR-10714, Dec. 1978.

AIAA 82-4007

Take-Off Ground Roll of Propeller Driven Aircraft

Roger J. Hawks*

Tri-State University, Angola, Ind.

Nomenclature

C_D	= drag coefficient
C_L	= lift coefficient
D	= reference length
g	= acceleration due to gravity
k	= induced drag factor, $C_D = C_{D_0} + kC_L^2$
m	= airplane mass
P	= effective thrust power
S	= wing area

Received Aug. 7, 1981. Copyright © American Institute of Aeronautics and Astronautics, Inc., 1981. All rights reserved.

*Associate Professor and Chairman, Department of Mechanical and Aerospace Engineering. Associate Fellow AIAA.

s_D	= aerodynamic penetration, $s_D = 2m/\rho S C_D$
s_L	= aerodynamic radius, $s_L = 2m/\rho S C_L$
T	= thrust
V	= speed
V_r	= reference speed
V_{TO}	= take-off speed
\bar{V}	= speed ratio, $\bar{V} = V/V_r$
W	= airplane weight
x	= ground roll distance
\bar{x}	= distance ratio, $\bar{x} = x/D$
μ	= coefficient of rolling resistance
ρ	= air density
ϕ	= airplane parameter

Introduction

IN aircraft performance analysis take-off ground roll calculations are usually performed numerically. In preliminary design, however, it is convenient to have available simple analytical techniques for estimating the take-off ground roll distance.

When the engine performance is expressed in terms of thrust the ground roll solution is well known.^{1,2} For engine thrust independent of airspeed the ground roll distance is

$$x = (1/2B) \ln [A / (A - BV_{TO}^2)] \quad (1)$$

where

$$A = g(T/W - \mu) \quad (2)$$

$$B = (C_D - \mu C_L) g \rho S / 2W \quad (3)$$

The ground roll is minimized when $C_D - \mu C_L$ is minimum or when

$$C_L = \mu / 2k \quad (4)$$

The solution given by Eqs. (1-3) does not apply to propeller driven aircraft since, in this case, the thrust-power, rather than the thrust, is constant. Thus the actual thrust will be inversely proportional to the speed. The solution to the acceleration problem for constant power with aerodynamic drag was first developed for automobile performance. Pershing³ considered only aerodynamic drag while Hawks and Sayre⁴ included both drag and lift in their analysis. In this Note the method of Ref. 4 will be applied to the take-off ground roll problem for propeller driven aircraft.

Theory

If we assume that the effective thrust-power of the engine-propeller combination is independent of airspeed the horizontal equation of motion for the airplane during ground roll (Fig. 1) is

$$mV \frac{dV}{dx} = \frac{P}{V} - \mu mg - \frac{1}{2} \rho S (C_D - \mu C_L) V^2 \quad (5)$$

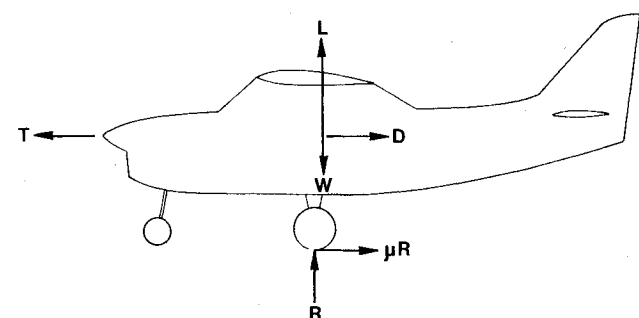


Fig. 1 Forces on aircraft in ground roll.